Available online at www.sciencedirect.com

SciVerse ScienceDirect

Journal of the European Ceramic Society 32 (2012) 1933–1940

www.elsevier.com/locate/jeurceramsoc

Processing, sintering and oxidation behavior of SiC fibers reinforced ZrB_2 composites

Diletta Sciti *, Laura Silvestroni

CNR-ISTEC, Institute of Science and Technology for Ceramics, Via Granarolo 64, I-48018 Faenza, Italy

Available online 25 November 2011

Abstract

Borides and carbides of early transition metals are considered a class of promising materials for several applications, the most appealing ones being in the aerospace and energy sectors. The present work is mostly focused on toughening of UHTCs through incorporation of SiC chopped fibers. Mechanical properties of reinforced composites are compared to those of un-reinforced, whisker- and particle-reinforced materials and the effect of different kinds of sintering aids is studied. Addition of fibers allows toughness to be increased from 3–4 MPa $m^{1/2}$ (for un-reinforced materials) to 5.0–6.2 MPa $m^{1/2}$. The high temperature behavior is also investigated both in air furnace and in arc jet facility. Eventually, a paragraph is dedicated to potential of UHTCs as sunlight absorbers for future solar concentrating systems operating in the high temperature regime.

Keywords: Borides; Composites; Fibres; Toughness and toughening; Corrosion

1. Introduction

Zirconium diboride-based materials are currently considered a class of promising materials for several applications, in particular in the aerospace sector. In the last five years, research has focused on the fabrication of dense composites possessing high strength (500–1000 MPa).[1–11] However, the low fracture toughness remains one of the major concerns for the application of these materials under severe environmental conditions. From data reported in the literature it is evident that often the addition of particles does not represent an effective strategy for a major toughness improvement. In case of SiC particles, for example, it has been shown that residual tensile stresses are developed in the ZrB_2 matrix, due to the difference of thermal expansion coefficient between SiC and ZrB_2.[7] As a result, particle-reinforced ZrB_2–SiC materials are often as brittle as other ZrB_2-based composites even if they display significant increase of hardness and strength.

Spherical reinforcement can be efficaciously substituted by elongated reinforcement. The potential advantages of elongated secondary phases over particulate-reinforced systems include more effective toughening mechanisms such as enhanced crack deflection and load-carrying capability. In addition, other toughening mechanisms, such as crack bridging and pullout, are possible. Indeed, significant increases of fracture toughness were obtained through addition of SiC whiskers,[12,13] carbon fibers[14] and more recently SiC chopped fibers.[15–17]

Oxidation of refractory diborides in air at elevated temperatures has limited their applications. One of the commonest additives used to improve the oxidation protection of ZrB_2 is silicon carbide[18–20] as it forms a coherent SiO_2-based glass layer on the surface of the ceramic. This continuous scale provides passive oxidation protection in the intermediate temperature regime (1100–1600 °C).

The aim of this work is to evaluate the efficacy of SiC chopped fibers as potential reinforcement for ZrB_2 analysing several aspects, such as: the impact of the sintering technique, the effect of the sintering aid, the high temperature stability, including both conventional tests in air furnace up to 1700 °C and arc jet tests to simulate re-entry conditions at temperatures exceeding 2000 °C. Furthermore, the performance of SiC fiber-reinforced composites is compared to that of whisker- or particle-reinforced composites at room, high temperature and in oxidising environment. Indeed, whether or not SiC chopped fibers can be as effective as SiC particles during oxidation is still an unexplored issue. A short paragraph at the end of the paper is dedicated to potential application of UHTCs in the solar energy sector.

* Corresponding author.
E-mail address: diletta.sciti@istec.cnr.it (D. Sciti).

0955-2219/$ – see front matter © 2011 Elsevier Ltd. All rights reserved.
doi:10.1016/j.jeurceramsoc.2011.10.032

2. Experimental

2.1. Preparation of SiC chopped fibers reinforced materials

Commercial raw materials were used to prepare the ceramic composites: ZrB_2 Grade B (H.C. Starck, Germany), particle size range 0.1–8 μm; SiC HI Nicalon chopped fibers, with composition (wt%) Si:C:O = 62:37:0.5. The dimensions are: 14 μm diameter, 1 mm length. As sintering additives the following powders were used in amount 5–10 vol%: α-Si_3N_4 Baysinid (Bayer, Germany); $ZrSi_2$-F (Japan New Metals Co., LTD, Osaka, Japan); $MoSi_2$ <2 μm (Aldrich, Steinbeim, Germany). The SiC fibers content varied from 0 to 30 vol%. Particular care needs to be paid for processing of fiber-reinforced materials. Homogenization of fibers and powders was accomplished by conventional ball milling for 24 using ZrO_2 media in absolute ethanol. However, compaction was generally more difficult than for conventional powder mixtures. The slurries were dried in a rotary evaporator and the powder mixtures underwent a slow debonding cycle in a graphite furnace at 500 °C for 60 min in flowing Argon. The powder–fiber mixtures were sintered in a graphite mould using a hot pressing machine at 1650, 1700 and 1750–1900 °C for compositions doped with $ZrSi_2$, Si_3N_4 and $MoSi_2$, respectively, with applied pressure of 40–50 MPa and holding time of 10 min. The microstructures were analyzed using scanning electron microscopy (SEM, Cambridge S360, Cambridge, UK) and energy dispersive spectroscopy (EDS, INCA Energy 300, Oxford instruments, UK) on fractured and polished surfaces. For comparison, SiC whisker- and particle-reinforced ZrB_2 composites were produced. Details on their preparation are given elsewhere.[11,15]

2.2. Mechanical characterization

Vickers microhardness (HV1.0) was measured by indentation with a 9.8 N load in a hardness tester Zwick model 3212. Fracture toughness (K_{Ic}) was evaluated using chevron notched beams (CNB) in flexure. The test bars, 25 mm × 2 mm × 2.5 mm (length by width by thickness, respectively), were notched with a 0.1 mm-thick diamond saw; the chevron-notch tip depth and average side length were about 0.12 and 0.80 of the bar thickness, respectively. The specimens were fractured using a semi-articulated silicon carbide four-point fixture with a lower span of 20 mm and an upper span of 10 mm on a universal testing machine Instron 1195. The specimens, three for each composite, were loaded with a crosshead speed of 0.05 mm/min. The "slice model" equation of Munz et al.[21] was used to calculate K_{Ic}. On the same machine and with the same fixture, the flexural strength (σ) was measured at room temperature and at 1200 °C in air.

2.3. High temperature characterization

The oxidation tests were carried out in a bottom-up loading furnace at 1200, 1500 and 1700 °C for 30 min in static air on various compositions containing either SiC chopped fibers or whiskers or particles. Specimens were located in the furnace when the maximum temperature was reached and then removed and air quenched after the exposure time. Mass and bars' dimensions were measured before and after the oxidation. Microstructural modifications induced by oxidation were analyzed by SEM-EDS. Flexural strength tests in four point fixture were conducted on 25 mm × 2 mm × 2.5 mm bars after oxidation at 1700 °C.

Arc jet tests: A composite containing 20 vol% fibers was selected for the realization of a sharp leading edge with a radius of curvature <0.5 mm. The experiments were conducted in an arc-jet plasma wind tunnel at the Department of Aerospace Engineering – University of Naples "Federico II", and involved high enthalpy supersonic flows in air with a nominal Mach number (M) around 3. The sharp wedge was locked upon an alumina holder at a distance of 10 mm from the nozzle exit. The surface temperature of the wedge was continuously measured by a two-colour pyrometer (Infratherm ISQ5, Impac Electronic GmbH, Germany) focused onto a position as close as possible to the edge of the sample. At the same time, the distribution of the surface temperature over the wedge was monitored using an infrared thermo-camera (FLIR Thermacam P40, spectral range 8–14 μm). Microstructural modifications induced by oxidation were then analyzed by SEM-EDS.

3. Results and discussion

3.1. Microstructure and properties of materials containing chopped fibers

For composites containing up to 20 vol% of fibers, few or no residual porosity was generally observed in the microstructure and the fiber dispersion into all the matrices was homogeneous, Fig. 1a. A significant fraction of residual porosity (∼8%) was noticed in the matrix containing 30 vol% of fibers (Fig. 1b), either in the boride matrix or at the matrix/fiber interface. It is apparent that increasing the reinforcement content makes increasingly difficult to properly process the powder mixtures to achieve a dense matrix and a good fiber dispersion. In all the composites a notable reduction of the fibers dimension (maximum length around 300 μm) was observed, due to both the action of milling media and the applied pressure during sintering. Secondary phases were observed in the sintered microstructures, including residual ZrO_2 particles, isolated pockets of BN, Zr–Si phases, SiO_2 and a borosilicate glass containing Zr–Si–B–N–O distributed along grain boundaries.[15,16] As for the fiber–matrix interface (Fig. 1c) it can be observed that a very complex system of reaction phases developed: around the original SiC fiber core, a Si–C–O rim was formed probably due to migration of intergranular phase towards the fiber surface. The latter often reacted with the liquid phase deriving from the sintering aids and/or gathered various impurities present in the matrix, especially ZrO_2. Fig. 1d shows the crack propagation features of these composites: the crack very often crosses the fibers without appreciable deviation due to the strong matrix/fiber interface.

The effect of SiC chopped fibers on mechanical properties of ZrB_2 composites is shown in Fig. 2 for the system containing Si_3N_4 as sintering agent. Fracture toughness was

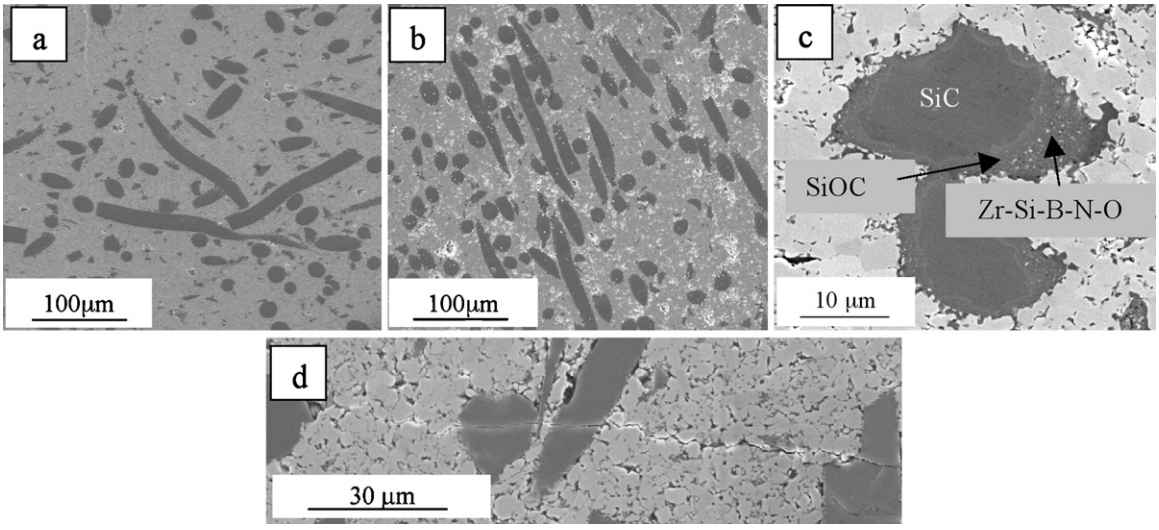

Fig. 1. $ZrB_2 + SiCf + Si_3N_4$ composites showing (a) typical microstructure of samples containing 20 vol% fiber, (b) typical microstructure of samples containing 30 vol% fiber, showing porosity in the boride matrix, (c) fiber/matrix interface, and (d) crack path obtained by a 9.8 N Vickers indentation.

improved significantly by the addition of fibers, up to 20 vol% (5.3 and 5.6 MPa $m^{0.5}$) in comparison with the reference materials (3.7 MPa $m^{0.5}$) (Fig. 2a). The toughness of a reinforced composite can be interpreted as the sum of the unreinforced matrix toughness plus the increment due to toughening mechanisms exerted by the fibers[15,16]:

$$K_{Ic}^{reinforced} = K_{Ic}^{matrix} + \Delta K^{fiber} \quad (1)$$

As crack propagation behavior displayed no pullout, deflection or bridging (Fig. 1c), it was concluded that the dominant toughening mechanism was crack bowing.[16] Beside this, a second toughening contribution deriving from thermal residual stresses was also considered, due to mismatch between thermal expansion coefficients and elastic constants of matrix and fibers.[22] As $\alpha_{SiC} < \alpha_{matrix}$, thermal residual stresses are expected to give a negative contribution to fracture toughness.[22] In previous works[16] it was shown that the toughening increment due to crack bowing[23] was much larger than the negative one from residual stresses that is almost negligible,[22] resulting in a net increase of toughness. Also, it was shown that this model is well suited for fiber content up to 20 vol% but fails for a higher content (30 vol%). Indeed, the residual porosity negatively affected both the matrix original toughness (K_{Ic}^{matrix}) and the reinforcing action of the fibers (ΔK^{fiber}).

The flexural strength of fiber-containing composites decreased from 600 to 400 MPa for 10–20 vol% fibers and 200 MPa for 30 vol% fibers (Fig. 2b). The incorporation of 200–300 μm long elements in a fine matrix (ZrB_2 mean grain size: 3 μm) very likely changed the defect population. Using the Griffith equation, $\sigma = 1.3\, K_{Ic}/C^{0.5}$, the size of the mean critical defect (C) was estimated to be about 100–200 μm, which suggests that fibers themselves could represent critical flaws. The flexural strength was also tested at 1200 °C in air (Fig. 2b). It can be observed that the composites nearly maintained the same *RT* value (~400 MPa). Furthermore, the composites were strengthened in comparison with the un-reinforced material that exhibited a value of 240 MPa at this temperature.

3.2. Effect of the sintering technique

Spark plasma sintering (SPS) is widely recognized as a very effective sintering technique that allows materials to be densified at lower temperatures and in a shorter time than in conventional sintering. Recent contributions have shown that this technique permits the successful densification of UHTC

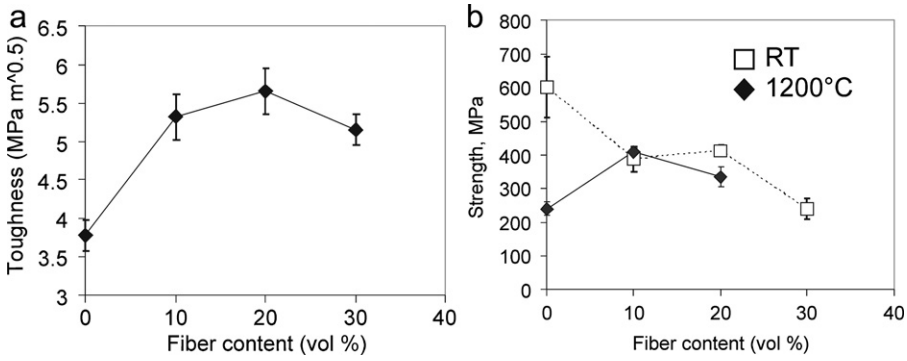

Fig. 2. Effect of the fiber content on (a) fracture toughness and (b) 4-pt flexural strength at room temperature and 1200 °C in air.

Table 1
Comparison of mechanical properties between compositions containing 20 vol% fiber and 5 vol% Si_3N_4, obtained by hot pressing (HP) and spark plasma sintering (SPS). K_{Ic}: fracture toughness by CNB, σ_{RT}: 4-pt flexural strength at room temperature, σ_{1200}: 4-pt flexural strength at 1200 °C.

Composition, vol%	Technique	T/t/P, °C/min/MPa	Exp. density, g/cm^3	K_{Ic}, MPa m$^{1/2}$	σ_{RT}, MPa	σ_{1200}, MPa	Ref.
ZrB_2 + 20 SiC fiber	HP	1700/10/50	5.2	5.65 ± 0.30	410 ± 20	340 ± 50	[15]
ZrB_2 + 20 SiC fiber	SPS	1500/5/50	4.7	5.53 ± 0.37	370 ± 20	447 ± 23	[16]

ceramics with reduced content of sintering aids[24,25] or with addition of phases (e.g. whiskers or fibers) that are very sensitive to degradation at high sintering temperatures.[13] As already mentioned, composites processed in ISTEC labs were sintered by hot pressing at 1700 °C. For comparison some SPS tests were conducted in Arrhenius Lab, Stockholm University, Sweden. The powder mixtures were sintered in an SPS furnace, in vacuum (5–10 Pa). The sintering temperature was in the range 1500–1700 °C and applied pressure was 50 MPa.[16] Microstructural analyses confirmed that composites containing 10–20 vol% fibers were completely dense at temperatures comparatively lower than for hot pressing, i.e. 1500 °C. However, despite the lower sintering temperature and lower holding time, microstructural analysis of the fiber–matrix interface confirmed a large extent of chemical interaction between SiC fibers, intergranular phases and ZrB_2. Mechanical properties of an SPS composite containing 20 vol% fiber are compared to those of the HP composite with the same composition in Table 1. The values of fracture toughness of the hot pressed composites were close to those of the SPS composites. This indicates that, even if a more efficient thermal treatment as SPS was used, the nature of the matrix/reinforcement interface did not change notably. In particular, the analysis of the interaction between an advancing crack and the microstructure confirmed that the intergranular wetting phases or interface reactions prevented any possibility of reinforcement pullout, independently of the sintering route. Also the strength values did not indicate substantial advantage of the SPS technique over the hot pressing route, at least for the composition tested.[16]

3.3. Effect of the shape of reinforcement (chopped fibers vs. whiskers and particles)

For the sake of comparison, SiC whisker- and particle-reinforced composites were produced by hot pressing at 1700 °C using the same sintering aid, Si_3N_4.[11,15] The mechanical properties of the three kind of composites containing 20 vol% of reinforcement are summarized in Table 2. Similar to the case of fiber additions, fracture toughness was improved by the addition of 20 vol% SiC whiskers (5.3 MPa m$^{0.5}$). However, incorporation of whiskers did not alter significantly the strength (~610 MPa).[15] The particle-reinforced composite had a lower toughness (4.6 MPa m$^{0.5}$) and higher strength (730 MPa), as expected. Concerning strength test at 1200 °C, it can be observed that for particle-reinforced composites, the strength decreased to 250 MPa, probably due to deleterious effects associated to softening of intergranular phases. In case of fiber and whisker additions, strength values were 340–350 MPa despite the presence of the same intergranular soft phases. The high-temperature strength is affected by several factors: a – softening of amorphous phases that causes a strength decrease; b – change of the defect population induced by oxidation, (the materials were kept about 30 min at a temperature >1000 °C) that causes a strength decrease; c – sealing of small porosities by the borosilicate glass, that could induce a strength increase. At 1200 °C, all the composites underwent effects a–c. The fact that whisker- and fiber-containing materials resulted in higher strength suggests that these reinforcing elements still have a strengthening effect. This, in turn, could be attributed to the fact that differently from particles, fibers and whiskers underwent a slower or incomplete oxidation and continued to exert a structural function.

3.4. Effect of sintering aid

The choice of sintering aid affects not only the sintering behavior of the matrix, but also the extent of reaction between matrix and fibers. A part from Si_3N_4, two silicides, namely $ZrSi_2$ and $MoSi_2$, were tested. The principle behind selection of these silicides is related to their efficacy in promoting the densification and in improving the oxidation resistance of boride matrices.[26] $ZrSi_2$ is a relatively low melting point phase (1600 °C) and thus densification was completed at 1600–1650 °C. For $MoSi_2$, that is more refractory, densification tests were carried out in the range 1750–1900 °C.[17] In all the cases dense composites were obtained. The analysis of the microstructure revealed that at similar densification temperatures, the addition of $MoSi_2$ promoted higher fiber degeneration in comparison with Si_3N_4 or $ZrSi_2$.

Table 2
Effect of the reinforcement type on mechanical properties of reinforced composites, K_{Ic}: fracture toughness by CNB, σ_{RT}: 4-pt flexural strength at room temperature, σ_{1200}: 4-pt flexural strength at 1200 °C, σ_{ret}: retained strength after oxidation at 1700 °C/30 min.

Composition, vol%	Reinforcement type	Additive, vol%	K_{Ic}, MPa m$^{1/2}$	σ_{RT}, MPa	σ_{1200}, MPa	Ref.	σ_{ret}, MPa
ZrB_2 + 20 SiC	Chopped fibers	Si_3N_4, 5%	5.65 ± 0.30	410 ± 20	340 ± 50	[15]	164 ± 8
ZrB_2 + 20 SiC	Whiskers	Si_3N_4, 5%	5.30 ± 0.30	614 ± 75	352 ± 22	[15]	180 ± 11
ZrB_2 + 20 SiC	Particles	Si_3N_4, 5%	4.55 ± 0.10	730 ± 100	250 ± 10	[11]	220 ± 22

Table 3
Effect of sintering aids on the mechanical properties. K_{Ic}: Fracture toughness by CNB, σ_{RT}: 4-pt flexural strength at room temperature.

Composition, vol%	Additive	Sintering temperature, °C	K_{Ic}, MPa m$^{0.5}$	σ_{RT}, MPa
ZrB_2	Si_3N_4	1700	3.7 ± 0.1	600 ± 90
ZrB_2 + 20 SiC fiber	Si_3N_4	1700	5.7 ± 0.3	410 ± 20
ZrB_2	$ZrSi_2$	1600	4.3 ± 0.1	808 ± 31
ZrB_2 + 20 SiC fiber	$ZrSi_2$	1600	6.2 ± 0.4	385 ± 13
ZrB_2	$MoSi_2$	1750	3.5 ± 0.6	780 ± 87
ZrB_2 + 20 SiC fiber	$MoSi_2$	1750	4.8 ± 0.1	380 ± 20
ZrB_2 + 20 SiC fiber	$MoSi_2$	1900	3.7 ± 0.3	–

Microstructural features are mirrored in the results of mechanical properties, reported in Table 3. Among the different systems, the maximum fracture toughness increase was for the composition containing $ZrSi_2$ as sintering additive, achieving 6.2 MPa m$^{0.5}$. No significant toughness increase was observed for $MoSi_2$ doped materials: the fibers degeneration occurring during sintering at 1900 °C rendered the reinforcements completely ineffective. A modest increase of toughness was instead found after sintering treatment at 1750 °C. As the toughness of the composites can be interpreted as the sum of the un-reinforced matrix toughness plus the increment due to toughening mechanisms exerted by the fibers (Eq. (1)), it can be stated that the higher toughness of the system containing $ZrSi_2$ is due to the higher toughness of its respective matrix. In the case of $MoSi_2$, the lowest values are both due to the lower toughness of the matrix and the fiber degeneration. Finally, one could observe that the change of sintering aid does not have a significant impact on the strength of the composites, being all values around 400 MPa.

3.5. Oxidation behavior

The oxidation tests were carried out in a bottom-up loading air furnace at 1200, 1500 and 1700 °C for 30 min on composites containing 20 vol% fibers. After oxidation at 1200 °C (not shown), a discontinuous cracked SiO_2 scale with ZrO_2 particles and damaged fibers was observed on the surface. After oxidation at 1500 and 1700 °C, islands of ZrO_2 in rounded particle or dendrite-like shape, were immersed in a SiO_2 continuous scale.[27] The polished sections of fiber-reinforced composites oxidised at 1500 and 1700 °C are reported in Fig. 3a and b and they generally followed the typical aspect of oxidised ZrB_2–SiC: an external SiO_2 layer, an intermediate coarse ZrO_2 partially filled with silica and a SiC-depleted layer above the unreacted bulk. No SiC-depleted layer is present in the materials after exposure at 1200 °C. After oxidation at 1500 °C carbon residuals were often observed around the fibers (Fig. 3c), which were hardly observed in oxidised SiC particle-reinforced ceramics.[28,29] This indicates that active oxidation of SiC fibers proceeds first through the reaction:

$$2SiC + O_2 = 2SiO\,(g) + 2C \quad (2)$$

instead of the more frequently reported reaction[28,29]:

$$SiC + O_2 = SiO\,(g) + CO\,(g) \quad (3)$$

It is interesting to study the effect of SiC reinforcement type on the oxidation behavior. When using chopped fibers, we introduce SiC elements with typical dimensions of 100–300 μm and diameter of 15 μm. The whiskers are typically 30 μm in length and diameter less than 1 μm. In composite containing particles, SiC particles tend to form agglomerates at triple points that do not overcome dimensions around 2–3 μm. In terms of weight gain, parallel oxidation experiments demonstrated that all the samples displayed similar values, in the range 1200–1700 °C.[27] However, when a depletion region is formed, in the case of fine SiC particles, a layer with small and fine porosity will form. In the case of fiber additions, the SiC depletion region will contain large cavities. An intermediate situation is represented by SiC whiskers. The strength degradation after oxidation at 1700 °C due to the surface modified layer is displayed in Table 2. As can be seen, the absolute value of retained strength is lower for the composite containing fibers (160 MPa) than for whiskers (180 MPa) and particles (220 MPa), confirming that morphology of the SiC phase can have a significant impact on the high temperature performance.

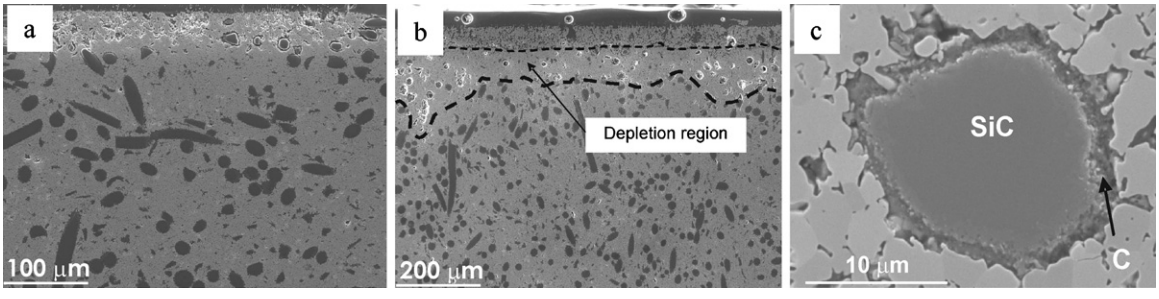

Fig. 3. Polished cross section of ZrB_2 + 20SiC fibers + Si_3N_4 after oxidation at (a) 1500 and (b) 1700 °C. (c) Initial stage of fiber oxidation.

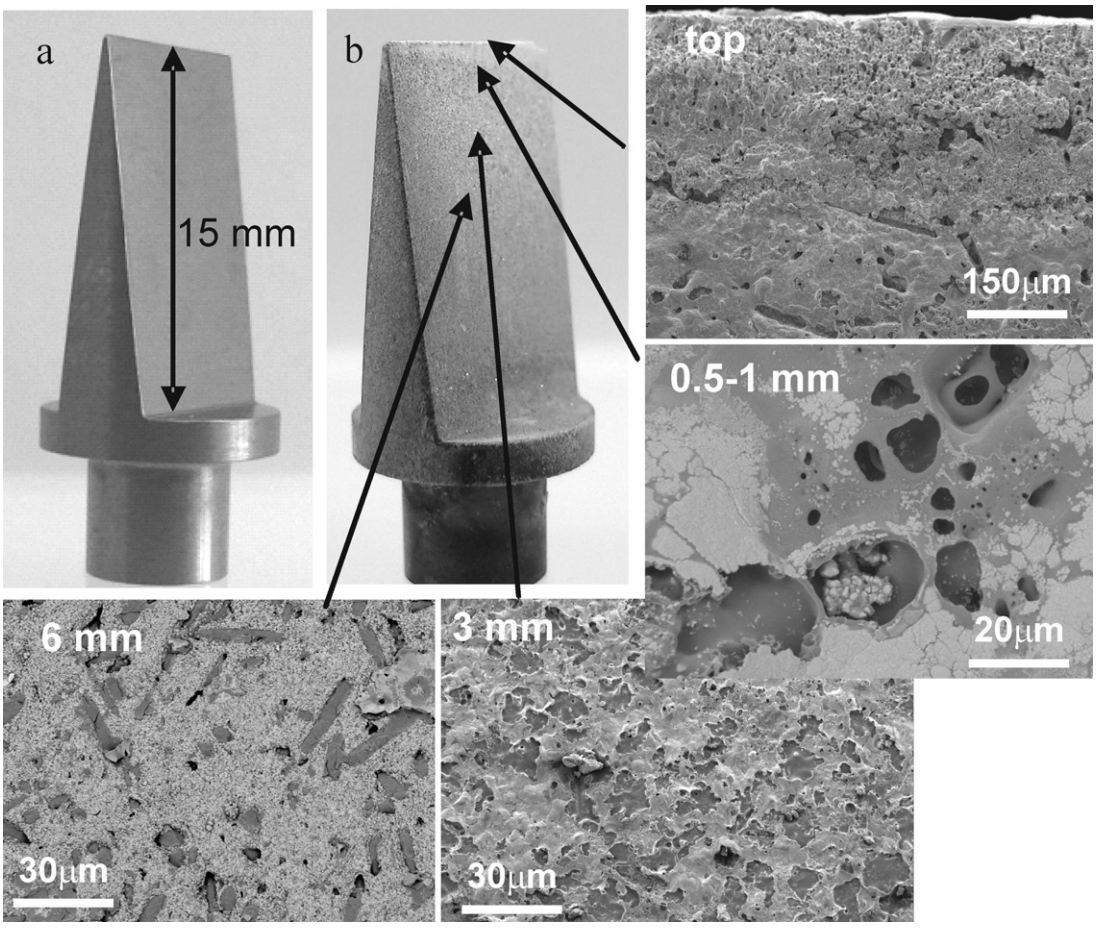

Fig. 4. External surface of the model (a) before and (b) after the arc-jet test with magnified areas of the modified microstructure.

3.6. Extreme oxidation behavior: arc-jet tests

The design of high-performance hypersonic vehicles requires pointed fuselage nose-cones and wing leading edges with very sharp profile, i.e. radius of curvature in the order of few millimeters. This helps the vehicle to enhance its performances and maneuvrability by reducing the drag and also to improve the crew safety due to an expanded down and cross-range capability.[30,31] However for sharp leading edges the convective heating to the surface, and hence the surface temperature, dramatically increases as the radius of curvature decreases.[31]

The composition containing 20 vol% fibers and silicon nitride was selected for the realization of a sharp leading edge with a radius of curvature less than 0.5 mm (Fig. 4a) to be tested in supersonic regime. The pyrometer was focused on a 3 mm diameter spot from the tip and the maximum average temperature reached in this region was 1700 °C. However, according to computational modeling, on the surface tip the temperature could reach values as high as 2300–2400 °C. The total time of exposition including heating ramps, was 17 min. Fig. 4a and b shows the appearance of the model before and after the test: the shape is maintained and the colour changed from white on the tip (presence of ZrO_2 phase) to black at the base (presence of silica-based glass). The most damaged area was obviously the summit of the sample where large cavities left by SiC fibers evaporation were well visible together with cracks (Fig. 4b). The presence of solely ZrO_2 phase was observed down to about 300 μm. Large pools of silica containing small ZrO_2 precipitates were visible at 400 μm from the surface and at 3 mm the predominant phase was zirconia and a discontinuous layer of silica. At 6 mm from the tip fibers were still recognizable, though cracked and damaged, among ZrO_2 particles. The cross section of the model was severely damaged by the polishing procedure (Fig. 5a). However the three typical regions observed for ZrB_2–SiC composites were recognizable: an outermost cracked zirconia layer (40 μm), a ZrB_2–SiO_2 interlayer (140 μm) and a SiC-depleted ZrB_2 region (400 μm thick). The appearance of SiC fibers was very similar to the morphology observed for other ZrB_2–SiC fibers composites oxidised in air furnace: the core was SiC which was oxygen enriched moving outside, around the fiber a continuous graphite layer was observed (see Fig. 3c). Although the effect of type of SiC reinforcement needs a more in-depth investigation, preliminary arc jet tests conducted on a composite containing 20 vol% SiC particles with the same geometry and in similar conditions did evidence a marked difference in the scale morphology (see Fig. 5b). In particular the scale shape is still sharp in the fiber-reinforced material and flattened in the particle-reinforced material, suggesting a different extent of ablation between the two composites. This behavior can be a

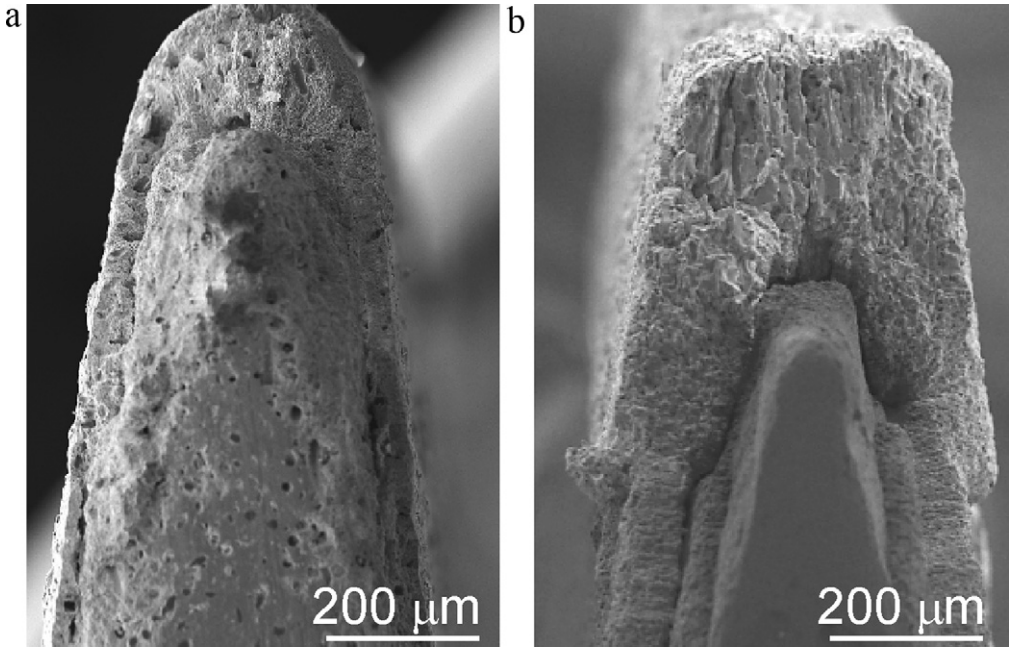

Fig. 5. Cross section of (a) SiC chopped fibers reinforced and (b) SiC particles reinforced ZrB_2.

consequence of a different oxidation rate of fibers and particles and will be object of future investigation.

4. UHTC for solar energy application

Beside the well known characteristics that make UHTCs attractive as thermal protection systems, there is a strong interest in their applications as sunlight absorbers for solar concentrating systems that can operate in the high temperature regime. Electricity generation from solar energy by thermo-mechanical conversion is currently limited in worldwide implementation, due to the relatively low conversion efficiency and the resulting high cost of the produced electricity. This level of performance and cost is achieved today in solar thermal power plant technologies that are based on steam cycles at moderate temperatures (400–550 °C). A real breakthrough may occur if the conversion efficiency from sunlight to electricity can be significantly increased. This would require heat input at temperatures in the range of 1000–1400 °C, which in turn faces significant challenges, especially concerning the key component that is the radiation absorber located at the focus of the concentrator field. The ideal absorber material should possess high emissivity in the solar spectrum (up to about 2 μm) and low emissivity outside this range to produce spectral selectivity, reasonable resistance to stresses, high thermal conductivity to smooth local hot spots due to uneven distribution of incident radiation and stability to chemical degradation caused by oxidation over long operation time at elevated temperature. Former materials used for volumetric absorbers include Al_2O_3, SiO_2 and SiC. Concerning UHTCs, there is some evidence that these composites possess a pronounced degree of intrinsic spectral selectivity,[32,33] however, the studies of spectral emissivity characteristics of UHTCs performed so far refer to films and coatings and not to bulk materials, either porous or dense.

For this reason a long-term investigation about UHTC potentialities as innovative absorber for new generation high-temperature concentrating solar power plants, CSP, has recently started in collaboration with the Italian Institute of National Optics (INO-CNR). Preliminary studies[34] have shown that borides and carbides behave very differently from conventional ceramics such as SiC. Even with some differences among them, all UHTCs display a step-like increase of reflectance from visible to infrared, with presence of a cut-off reflectance wavelength. These characteristics, in combination with other key properties as high thermal and electrical conductivities, superior oxidation resistance up to 1600 °C make unreinforced UHTC monoliths and composites particularly interesting for solar applications. Further studies will be devoted to investigation of high temperature optical behavior up to 1200 °C or higher.

5. Conclusions and final remarks

The addition of SiC chopped fibers has demonstrated to be a viable method for improving the fracture toughness of brittle ZrB_2 ceramics as values of 5.7–6.2 MPa $m^{1/2}$ can be reached for compositions containing 20 vol% fibers. As far as oxidation is concerned the stability of fiber-reinforced composites is comparable to that of SiC particles reinforced composites, either in air furnaces up to 1700 °C or in arc jet tests from 1700 to 2400 °C, at Mach 3. One drawback for these composites is the decrease of flexural strength which passes from typical 700–800 MPa for un-reinforced or particle reinforced materials to 400 MPa for compositions with 10–20 vol% of fibers. However, it should be mentioned that for strength tests at high temperature (at least up to 1200 °C), flexural strength is presently higher than that of several developed ZrB_2-based materials. It was shown that the choice of the sintering aid is a key issue, as it affects not only the matrix sintering temperature, but also the reactivity

between matrix and fiber. In turn, the presence of secondary phases deriving from sintering aid can severely affect the high temperature mechanical and thermal performance. Among the possible options, silicon nitride was found to offer the best compromise. Future directions for increasing UHTCs performance include:

- minimization of sintering aid amount for improving high temperature performance up to 1500 °C;
- minimization of *RT* strength deterioration (optimization of fiber amount and material processing);
- improvement of thermal shock resistance.

Finally, un-reinforced UHTCs can find a novel field of application as solar absorbers, due to their intrinsic spectral selectivity that is possessed only by a limited number of materials. These characteristics, in combination with other key properties as high thermal and electrical conductivities, superior oxidation resistance make UHTC monoliths and composites particularly attractive for high temperature solar applications.

Acknowledgements

Authors wish to acknowledge R. Savino for arc jet tests (University of Naples "Federico II", Napoli, Italy); M. Nygren for SPS tests (Arrhenius lab, Stockolm University, Stockolm, Sweden); E. Sani and L. Mercatelli for optical tests (Institute of National Optics, INO-CNR, Firenze, Italy); S. Guicciardi and C. Melandri for mechanical test and discussion; D. Dalle Fabbriche for the hot pressing and oxidation routes.

References

1. Gasch MJ, Ellerby DT, Johnson SM. Ultra high temperature ceramic composites. In: Bansal NP, editor. *Handbook of ceramic composites*. Boston: Kluwer Academic Publishers; 2005. p. 197–224.
2. Fahrenholtz WG, Hilmas GE, Talmy IG, Zaykoski JA. Refractory diborides of zirconium and hafnium. *J Am Ceram Soc* 2007;**90**(5):1347–64.
3. Telle R, Sigl LS, Takagi K. Boride-based hard materials. In: Riedel R, editor. *Handbook of ceramic hard materials*. Weinheim, Germany: Wiley-VCH; 2000. p. 802–945.
4. Cutler RA. Engineering properties of borides. In: Schneider Jr SJ, editor. *Ceramics and glasses: engineered materials handbook*, vol. 4. Materials Park, OH: ASM International; 1991. p. 787–803.
5. Levine SR, Opila EJ, Halbig MC, Kiser JD, Singh M, Salem JA. Evaluation of ultra-high temperature ceramics for aeropropulsion use. *J Eur Ceram Soc* 2002;**22**:14–5, 2757–67.
6. Chamberlain AL, Fahrenholtz WG, Hilmas GE. High-strength zirconium diboride-based ceramics. *J Am Ceram Soc* 2004;**87**(6):1170–2.
7. Watts J, Hilmas GE, Farenholtz WG, Brown D, Clausen B. Stress measurements in ZrB_2–SiC composites using Raman spectroscopy and neutron diffraction. *J Eur Ceram Soc* 2010;**30**:2165–71.
8. Sciti D, Guicciardi S, Bellosi A, Pezzotti G. Properties of a pressureless-sintered ZrB_2–$MoSi_2$ ceramic composite. *J Am Ceram Soc* 2006;**89**:2320–2.
9. Balbo A, Sciti D. Spark plasma sintering and hot pressing of ZrB_2–$MoSi_2$ ultra-high-temperature ceramics. *Mater Sci Eng A* 2008;**475**:108–12.
10. Sciti D, Silvestroni L, Celotti G, Melandri C, Guicciardi S. Sintering and mechanical properties of ZrB_2–$TaSi_2$ and HfB_2–$TaSi_2$ ceramic composites. *J Am Ceram Soc* 2008;**91**:3285–91.
11. Monteverde F, Guicciardi S, Bellosi A. Advanced in microstructure and mechanical properties of zirconium diboride based ceramics. *Mater Sci Eng A* 2003;**346**:310–9.
12. Zhang P, Hu P, Zhang X, Han J, Meng S. Processing and characterization of ZrB_2–SiCw ultra-high temperature ceramics. *J Alloys Compd* 2008;**472**:358–62.
13. Wang H, Wang CA, Yao X, Fang D. Processing and mechanical properties of zirconium diboride-based ceramics prepared by spark plasma sintering. *J Am Ceram Soc* 2007;**90**:1992–7.
14. Yang F, Zhang X, Han J, Du S. Characterization of hot-pressed short carbon fiber reinforced ZrB_2–SiC ultra-high temperature ceramic composites. *J Alloys Compd* 2009;**472**:395–9.
15. Silvestroni L, Sciti D, Guicciardi S, Melandri C. Toughened ZrB_2-based ceramics with addition of SiC whiskers or chopped fibres. *J Eur Ceram Soc* 2010;**30**:2155–64.
16. Guicciardi S, Silvestroni L, Nygren M, Sciti D. Microstructure and toughening mechanisms in spark plasma sintered ZrB_2 ceramics reinforced by SiC whiskers or SiC chopped fibers. *J Am Ceram Soc* 2010;**93**(8): 2384–91.
17. Sciti D, Guicciardi S, Silvestroni L. SiC chopped fibers reinforced ZrB_2: effect of the sintering aid. *Scr Mater* 2011;**64**:769–72.
18. Shaffer PTB. An oxidation resistant boride composition. *Am Ceram Bull* 1962;**41**(2):96–9.
19. Tripp WC, Davis HH, Graham HC. Effect of an SiC addition on the oxidation of ZrB_2. *Am Ceram Bull* 1973;**52**(8):612–6.
20. Rezaie A, Fahrenholtz WG, Hilmas GE. Evolution of structure during the oxidation of zirconium diboride–silicon carbide in air up to 1500 °C. *J Eur Ceram Soc* 2007;**27**(6):2495–501.
21. Munz DG, Shannon Jr JL, Bubsey RT. Fracture toughness calculations from maximum load in four point bend tests of chevron notch specimens. *Int J Fracture* 1980;**16**:R137–41.
22. Taya M, Hayashi S, Kobayashi AS, Yoon HS. Toughening of a particulate-reinforced ceramic–matrix composite by thermal residual stress. *J Am Ceram Soc* 1990;**73**:1382–91.
23. Rouxel T, Laurent Y. Fracture characteristics of SiC particle reinforced oxynitride glass using chevron-notch three-point bend specimens. *Int J Fracture* 1998;**91**:83–101.
24. Sciti D, Silvestroni L, Nygren M. Spark plasma sintering of Zr- and Hf-borides with decreasing amounts of $MoSi_2$ as sintering aid. *J Eur Ceram Soc* 2008;**28**:1287–96.
25. Sciti D, Guicciardi S, Nygren M. Densification and mechanical behavior of HfC and HfB_2 fabricated by spark plasma sintering. *J Am Ceram Soc* 2008;**91**:1433–40.
26. Sciti D, Brach M, Bellosi A. Long-term oxidation behavior and mechanical strength degradation of a pressureless sintered ZrB_2–$MoSi_2$ ceramic. *Scr Mater* 2005;**53**:1297–302.
27. Silvestroni L, Sciti D. Oxidation of ZrB_2 ceramics containing SiC as particles, whiskers, or short fibers. *J Am Ceram Soc* 2011;**94**(9):2796–9.
28. Fahrenholtz WG. Thermodynamic analysis of ZrB_2–SiC oxidation: formation of a SiC-depleted region. *J Am Ceram Soc* 2007;**90**(1): 143–8.
29. Monteverde F, Bellosi A. Oxidation of ZrB_2-based ceramics in dry air. *J Electrochem Soc* 2003;**150**(11):B552–9.
30. Squire T, Marschall J. Material property requirements for analysis and design of UHTC components in hypersonic applications. *J Eur Ceram Soc* 2010;**30**:2239–51.
31. Monti R, Savino R, De Stefano Fumo M. Matching flight conditions on sharp leading edges in plasma wind tunnels. *J Thermophys Heat Transfer* 2007;**21**(3):660–4.
32. Bogaerts WF, Lampert CM. Review, Materials for photothermal solar energy conversion. *J Mater Sci* 1983;**18**:2847–75.
33. Kennedy CECE. *Review of mid-to high-temperature solar selective absorbers materials*. National Renewable Energy Laboratory; 2002.
34. Sani E, Mercatelli L, Sansoni P, Silvestroni L, Sciti D. Ultra-high temperature ceramic absorbers for high-temperature thermodynamic solar plants. *J Renew Sustain Energy*, submitted for publication.